# Screening of effective parts of She Medicine Xiaoxianggou and studying its mechanism in the treatment of gouty arthritis

**Yulong Huang**
Ningde Clinical College of Fujian Medical University
**Xiaohui Lin**
Ningde Clinical College of Fujian Medical University
**Minhua Lin**
Ningde Clinical College of Fujian Medical University
**Reheman Aikebaier**
Ningde Normal University
**Yujia Wang**
Ningde Clinical College of Fujian Medical University
**Di Zhong**
The Graduate School of Fujian Medical University
**Bingying Xiao**
The Graduate School of Fujian Medical University
**Jiangyuan Zhang**
Ningde Clinical College of Fujian Medical University
**Lingling Zhang**
Ningde Clinical College of Fujian Medical University
**Zichun Chen**
Ningde Clinical College of Fujian Medical University
**Xuekun Nie**
niexuekun@ndnu.edu.cn

Ningde Clinical College of Fujian Medical University

**Research Article**

**Keywords:** Traditional She medicine, Xiaoxianggou, RAW264.7 inflammatory cells, TLR4/MYD88 signaling pathway, gouty arthritis

**Posted Date:** February 15th, 2024

**DOI:** https://doi.org/10.21203/rs.3.rs-3951391/v1



**Additional Declarations:** No competing interests reported.

# Abstract

The prevalence of gouty arthritis has been steadily rising over recent years, with a trend towards an earlier onset. Currently, the main drugs used in clinical practice for the treatment of gouty arthritis include non-steroidal anti-inflammatory drugs and glucocorticoids. However, these drugs come with certain limitations, including low efficacy, side effects, and a high risk of palindromia. Xiaoxianggou, a traditional medicine, is derived from the dried roots and stems of Ficus pandurata Hance var. angustifolia Cheng or Ficus pandurata Hance var. holophylla Migo. It has properties such as wind elimination, dampness removal, heat-clearing, and detoxification. Notably, Xiaoxianggou exhibits a superior therapeutic effect on gout arthritis, although its mechanism of action remains unclear.

**Objective** To investigate the extraction process of Xiaoxianggou and improve its potential as a treatment for GA, it is essential to screen the active site and validate its effectiveness through cellular and animal studies to explore its potential mechanism.

**Method** The ultrasonic-assisted extraction of total phenols from Xiaoxianggou was optimized using an orthogonal experimental design. The MTS method was employed to determine the optimum concentration of the anti-inflammatory drug in Xiaoxianggou. ELISA was utilized to assess the levels of IL-1β and TNF-α in a macrophage inflammation model and synovial tissue of rats. The therapeutic effect of Xiaoxianggou's ethyl acetate fraction on GA rats was evaluated based on joint swelling and gait behavior scores. Joint tissue pathologies in GA rats were observed through hematoxylin-eosin (HE) staining. The main chemical components of Xiaoxianggou's ethyl acetate fraction were analyzed using HPLC-MS/MS technology. The network pharmacology approach was employed to identify potential signaling pathways associated with the treatment of GA using Xiaoxianggou's ethyl acetate fraction. TLR4/MYD88 pathway-related mRNA expression in the RAW264.7 cell inflammatory model treated with Xiaoxianggou's ethyl acetate fraction was determined using real-time fluorescence quantitative PCR.

**Result** The optimal extraction conditions for total phenols from Xiaoxianggou were determined to be a temperature of 70 ℃, an ethanol volume fraction of 60%, and a material-liquid ratio of 1:30. The ethyl acetate effective part of Xiaoxianggou demonstrated the ability to decrease the expression of TNF-α in RAW264.7 cells. Furthermore, it was found that Xiaoxianggou ethyl acetate effective part can reduce the expression of TNF-α and IL-1β in rats suffering from gouty arthritis, while also improving the histopathological structural changes in joint synovium. Moreover, the ethyl acetate effective parts of Xiaoxianggou reduced the mRNA expression of genes associated with the TLR4/MYD88 pathway in inflammatory cell models of RAW264.7.

**Conclusion** The effective component of ethyl acetate, Xiaoxianggou, exhibits a specific therapeutic effect on GA. Its mechanism of action is correlated with the TLR4/MYD88 signaling pathway.


# 1. Introduction

Xiaoxianggou, also known as Xiaokangbu, is a dried root and stem derived from two variations of *Ficus pandurata* Hance var. *angustifolia* Cheng or *Ficus pandurata* Hance var. *holophylla Migo.* It is a traditional medicinal herb used primarily by the She nationality and distributed in Fujian and Zhejiang provinces [1]. Xiaoxianggou is known for its effectiveness in dispelling wind and dampness, strengthening the spleen, and stopping diarrhea. It is widely used in folklore to treat joint pain, gout, and hepatitis [2]. Recent pharmacological studies have shown that Xiaoxianggou possesses numerous activities, such as scavenging free radicals [3], inhibiting xanthine oxidase [4] and anti-atherosclerosis [5]. These activities may be attributed to its high content of polyphenolic compounds [6]. The chemical structure of polyphenols includes phenolic hydroxyl groups that are highly susceptible to oxidation. These groups contribute to the strong antioxidant and free radical scavenging abilities of polyphenols. Additionally, polyphenols can act as multi-group ligands, chelating metal ions and inhibiting corresponding metalloenzymatic activities. This characteristic is crucial in demonstrating the antiviral and antimicrobial effects of polyphenols [7]. Consequently, polyphenols have emerged as a significant area of interest for natural drug development.

Gouty arthritis is a metabolic disease characterized by inflammation caused by the deposition of sodium urate crystals in the joints and the surrounding soft tissues. This condition arises from chronically elevated levels of uric acid in the body. If left untreated, it can cause joint damage and lead to complications such as gouty nephritis, kidney stones, uremia, hypertension, and other severe conditions that significantly impact patients' quality of life [8]. Previous research has indicated a higher prevalence of gout among older individuals compared to younger populations. However, due to improvements in living standards and dietary habits, there is an increasing incidence of gout in younger age groups [9]. The initial presentation of gout manifests as acute joint inflammation, predominantly affecting the lower extremities. Typically, this inflammation subsides within 7–14 days [10]. If recurrent acute gout episodes persist over an extended period, they can progress to chronic gout.

The pathogenesis of gout remains incompletely understood; however, there is a consensus that the disease follows a sequence of four pathophysiological stages: onset of hyperuricemia, deposition of MSU crystals in the joint tissue, the acute inflammatory response at the site of crystal deposition, and the eventual development of advanced clinical manifestations characterized by gout stones [11]. MSU crystals, as pathogen-associated molecules, can be recognized by macrophages and monocytes in the body's innate immune system, leading to the production of the nucleotide-binding oligomerized structural domain-like receptor protein 3 (NLRP3) inflammatory complex that initiates the pathological process of gout [12]. The activation of NLRP3 inflammatory vesicles can occur through two main pathways. The first pathway involves MSU crystals recognizing Toll-like receptors (TLR) of macrophages and activating nuclear transcription factor-κB (NF-κB) via the myeloid differentiation factor 88 (MyD88) pathway. This process promotes the formation of the NLRP3 inflammatory complex and releases inflammatory factors such as TNF-α and IL-1β. The second pathway occurs when macrophages phagocytose MSU crystals directly, resulting in the assembly of NLRP3 inflammatory vesicles and subsequent activation of caspase-1. Caspase-1 cleaves the precursor IL-1β protein into its mature form, IL-1β bodies [13, 14]. The produced IL-

1β binds to receptors of inflammatory factors, leading to the expression of chemokines and other molecules that regulate inflammation. This process triggers inflammatory responses, such as redness, swelling, heat, and increased vascular permeability at the injury site [8, 15]. To investigate the role of the TLR/MYD88 signaling pathway in gouty arthritis, Shen Ruiming et al. [16–18] administered traditional Chinese medicine (TCM) to GA mice. The results indicated that the expression of molecules related to the TLR/MYD88 signaling pathway increased, and there were significant inflammatory histopathological changes in the model group. In contrast, the treatment group showed a reduced expression of TLR/MYD88 signaling pathway-related molecules to varying degrees, indicating that the TLR/MYD88 signaling pathway may play a crucial role in the pathogenesis and drug treatment of GA. Therefore, targeting the TLR/MYD88 signaling pathway for inhibition could be essential in the drug treatment of GA.

The main drugs used in the clinical treatment of GA, such as colchicine, non-steroidal anti-inflammatory drugs (NSAIDs), glucocorticoids during the acute phase, or uric acid-lowering drugs throughout the chronic phase, often impose limitations in clinical application due to their numerous side effects, potential harm to liver and kidney function, and the inclination for relapse following discontinuation. However, traditional Chinese medicine has a lengthy history of addressing gout and classifies it as a form of paralysis. According to the dialectical method of TCM, acute attacks of gout are typically caused by the buildup of damp heat and can be treated using medicinal substances such as rhubarb and Datura, which possess heat-clearing, detoxifying, and pain-relieving qualities [19]. TCM has been evidenced to hinder gout attacks and ameliorate joint lesions by diminishing inflammatory mediators and bolstering the body's resistance to oxidative stress [20–22]. However, research progress in this field could be faster due to the complexity of the herbal components and extraction processes involved [23]. While Xiaoxianggou has demonstrated clinical efficacy and safety in GA treatment, further research is needed to explore its underlying pharmacological substances and potential mechanisms [24–25]. Therefore, elucidating the site of action and pharmacological mechanism of Xiaoxianggou in treating GA can present innovative options and strategies for the prevention and treatment of GA.

The objective of this study is to utilize the RAW264.7 macrophage inflammation model to select the optimal extraction process to screen for the effective site of the anti-inflammatory properties of Xiaoxianggou. Furthermore, a rat model of GA was established to validate the anti-inflammatory effect of Xiaoxianggou. The pharmacological active ingredients and potential mechanisms of Xiaoxianggou's anti-GA effect were analyzed using LC-MS and network pharmacology techniques. In addition, a preliminary experimental validation was conducted on key target genes to provide a theoretical foundation for promoting the development and application of Xiao Xiang Gou, a national drug.

# 2. Materials and methods

# 2.1 Cells

The mouse macrophage cell line RAW264.7 was purchased from the Cell Bank of the Typical Culture Repository Committee of the Chinese Academy of Sciences.

## 2.2 Animals

Six-week-old SD rats with SPF grade were obtained from the Institute of Medical Laboratory Animals, Chinese Academy of Medical Sciences (license No. SCXK [Beijing] 2019-0008) and individually housed in cages with ad libitum access to food and water. The rats were kept at a constant ambient temperature of (22 ± 2) ℃ and subjected to a 12-hour light-dark cycle. Prior to the experiment, the SD rats were acclimated to the experimental environment for one week. The animal experiments were approved by the ethics committee of Ningde Hospital affiliated with Ningde Normal College.

## 2.3 Medicinal materials

The Xiaoxianggou of She Medicine was acquired from the demonstration base of She medicine cultivation in Beishan Village, Jiaocheng District, Ningde City. Lan Fulu, the vice president of Min Dong She Chinese Herbal Medicine Association, authenticated it. The herbs were carefully dried, crushed, and sifted using an 80 mesh sieve.

## 2.4 Main regents

Gallic acid control (lot no. G823638), Folin-Ciocalteu reagent (lot no. P824172), anhydrous sodium carbonate (analytical purity), sodium urate (U886060-5g), and sodium hydroxide (analytical purity) were all purchased from Shanghai Maclean Biochemical Technology Co. Anhydrous ethanol (analytical purity), ethyl acetate, chloroform, and isopropanol (170802) were obtained from Xilong Science Co. Concentrated hydrochloric acid (T622-1989) was purchased from Chenghai Chemical Industry in Shanghai. DMEM medium (D6419-500mL) was acquired from Sigma, while fetal bovine serum (PS-FB5-SA) was obtained from Hyclone in the USA. Penicillin-Streptomycin Solution 100X (C0222), Glutamax (35050061), Sodium Pyruvate 100 mM Solution (11360070), and 0.25% Trypsin (25200-056) were purchased from Beyotime, Shanghai, Invitrogen, USA, and Gibco, USA, respectively. PBS buffer (PB180327) was obtained from Procell in Wuhan. Mouse TNF-α (Tumor Necrosis Factor Alpha) ELISA Kit (E-EL-M3063), MTS kit (G3581), GoScript Reverse Transcription Mix, Oligo(dT) (A2791), Eastep qPCR Master Mix (LS2062), and DMSO (219605580) were purchased from Elabscience, Promega, USA, and MP Biomedicals, USA, respectively. Rat TNF-α ELISA Kit (EK0526) and Rat IL-1 beta ELISA Kit (EK0393) were obtained from Wuhan Boster Biological Technology Co. Fisher Chemical supplied acetonitrile (ACN), formic acid (FA), and methanol. TRNzol total RNA extraction reagent (DP424) was purchased from TIANGEN in Beijing. Lastly, Mouse GAPDH internal reference primer, 10 μM (B661304), was acquired from Bioengineering, Shanghai.

## 2.5 Technology optimization of extraction process from Xiaoxianggou

The total phenols from Xiaoxianggou were extracted using the ultrasonic extraction method. Prior to the extraction process, the dried powder was soaked in an appropriate amount of solvent for one hour. The study consisted of examining various factors, including extraction time (10, 20, 30, 40, 50, 60 min, n = 3),

volume fraction of ethanol (30%, 40%, 50%, 60%, 70%, 80%, 90%, n = 3), material-liquid ratio (1:20, 1. 30, 1:40, 1:50, n = 3), extraction times (1, 2, 3 times, n = 3), and extraction temperatures (30, 40, 50, 60, 70, 80 ℃, n = 3). Each factor was tested at different levels, and the results were analyzed using an orthogonal test. The optimal extraction conditions were determined using extreme difference analysis. The L9 (33) orthogonal table optimized the ultrasonic extraction process. The study focused on three factors: extraction temperature (A), ethanol volume fraction (B), and material-to-liquid ratio (C), each with three selection levels (Table 1).

Table 1
Ultrasonic-assisted extraction of total phenols L9($3^3$) from Xiaoxianggou

| Level | Factor | | |
|---|---|---|---|
| | A Temperature(℃) | B Ethanol volume fractio(%) | C Material to liquid ratio(g/mL) |
| 1 | 60 | 60 | 1:20 |
| 2 | 70 | 70 | 1:30 |
| 3 | 80 | 80 | 1:40 |

# 2.6 Preparation of effective parts of Xiaoxianggou

The alcoholic extract was obtained using an optimized extraction process. T Ethanol was evaporated from the extract, and the resulting solution was then sequentially extracted with ethyl acetate and n-butanol. Subsequently, the obtained extracts of Xiaoxianggou were freeze-dried using rotary evaporation to yield lyophilized powders of ethyl acetate, n-butanol, and water extracts. These powders were subsequently dissolved in DMSO to generate mother liquors of different concentrations.

# 2.7 Cell viability assay by MTS

RAW264.7 cells were cultured in DMEM high sugar medium supplemented with 10% FBS, 1% double antibodies (penicillin, streptomycin), 1% glutamine, and 1% sodium pyruvate. The cells were incubated in a cell culture incubator at a constant temperature of 37 ℃ with a $CO_2$ concentration of 5%. The cells were seeded in 96-well plates at a density of $1\times10^4$ cells per well. After 24 hours of incubation, the cells were divided into control group, DMSO solvent control group, Xiaoxianggou ethyl acetate phase (10, 20, 40, 80, 120, 160, 200 μg/mL), Xiaoxianggou n-butanol phase (10, 20, 40, 80, 120, 160, 200 μg/mL), and Xiaoxianggou water phase (100, 200, 400, 600, 800, 1000 μg/mL). The blank control and DMSO solvent control groups were treated with serum-free DMEM high sugar medium alone, while the drug-treated group was exposed to the corresponding concentration of drug-containing medium. Following an additional incubation period of 6 hours at 37 ℃, the supernatant was removed from each group. The control group was then subjected to serum-free DMEM medium, and the other groups were exposed to DMEM high sugar medium containing MSU at a concentration of 400 μg/mL for 24 hours. After discarding the supernatant again, each group was treated with 100 μL of DMEM medium and 20 μL of

MTS. The absorbance of each well was measured at 490 nm after an incubation period of 2–3 hours, while ensuring protection from light.

## 2.8 Detection of cellular inflammatory factor expression levels by ELISA

After incubation for 24 hours, the cells were divided into blank control, model, and drug-treated groups. The drug-treated groups were exposed to varying concentrations of Xiaoxianggou ethyl acetate phase (10, 20, 40 μg/mL), Xiaoxianggou n-butanol phase (10, 20, 40 μg/mL), and Xiaoxianggou water phase (100, 200, 400 μg/mL). The blank control and model groups received serum-free DMEM high sugar medium, while the drug-treated group received corresponding concentrations of medium containing the drug. The cells were incubated for 6 hours at 37 ℃ in different groups. The control group was replaced with serum-free DMEM culture medium, while the remaining groups were replaced with DMEM high sugar medium containing MSU 400 μg/mL for 24 hours. After incubation, the supernatant was removed and discarded, and the cell supernatant was collected to measure TNF-α. The expression level of the inflammatory factor TNF-α was determined using a kit and following the provided instructions.

## 2.9 Detection of TLR4, MYD88, NF-κB, TNF-α and IL-1β mRNA gene expression by qRT-PCR

RAW264.7 cells were seeded at a density of $3x10^5$ cells/mL in 60-mm culture dishes. Total RNA was extracted using the TRIzol method, and subsequently, the concentration and purity of the total RNA were assessed. A kit was used to reverse transcribe 5 μg of RNA into cDNA. The qRT-PCR reaction was then conducted, with cDNA serving as the template, following the instructions provided by the kit manufacturer. The $2^{-\Delta\Delta Ct}$ method was used to calculate the relative expression of the target gene with GAPDH as the internal reference. Shanghai Sangon Biotech synthesized PCR primers; their sequences can be found in Table 2.

Table 2
PCR primer sequence

| Genes | | Primer sequence (5'→3') |
|---|---|---|
| *TLR-4* | Forward | AATGAGGACTGGGTGAGAAATG |
| | Reverse | GCAATGGCTACACCAGGAATA |
| MYD88 | Forward | AGCAGAACCAGGAGTCCGAGAAG |
| | Reverse | GGGCAGTAGCAGATAAAGGCATCG |
| *NF-κB* | Forward | GGGGATGTGAAGATGTTGC |
| | Reverse | GGATGATGGCTAAGTGTAAGA |
| *IL-1β* | Forward | CACTACAGGCTCCGAGATGAACAAC |
| | Reverse | TGTCGTTGCTTGGTTCTCCTTGTAC |
| *TNF-α* | Forward | ATGTCTCAGCCTCTTCTCATTC GCTTGTCACTCGAATTTTGAGA |
| | Reverse | |

# 2.10 Animal experimental grouping, labeling and drug administration

A total of 48 six-week-old SD rats were used in the study after being acclimatized for one week. These rats were randomly assigned to six different groups: normal, model, positive control (colchicine 0.3 mg/kg), and Xiaoxianggou ethyl acetate effective part treatment group [3.125, 6.25,12.5 g/(kg-d)]. The dosages for the treatment groups were determined based on the conversion factors for human and animal subjects as described in "Pharmacological Experimental Methodology," edited by Prof. Wei. Each group consisted of 8 rats, and to keep track of each rat, an ear tag method was used for labeling and recording. After 1 week of adaptive feeding, the drug was administered orally through gavage for 7 consecutive days. The blank and model groups received an equal volume of saline solution through gavage.

# 2.11 Establishment of gouty arthritis rat model

On the fifth day of gavage administration, we selected the lateral posterior aspect of the right hind ankle joint as the puncture site. Prior to the puncture, the ankle joint of each rat was disinfected using an iodophor. Subsequently, a No. 4 needle was employed to inject 100 μL of MSU solution (25 mg/mL) into the joint cavity, angled downward at approximately 30–40° along the medial aspect of the Achilles tendon. The standard injection resulted in tympanism on the opposite side of the rat's joint capsule. In the control group, the same dose of normal saline was injected using the same procedure.

# 2.12 Scoring of the degree of joint swelling

To minimize interference with the measured values, the fur of the rats was shaved precisely 3 mm above and below the right hind ankle joint. Additionally, a marker was positioned 1 mm below the joint to demarcate the area of interest. To establish the model, sodium urate solution was injected into the ankle joint, and the circumference of the marked area was subsequently measured at specific time intervals before the injection and at 1, 12, 24, and 48 hours post-injection. Each measurement was meticulously repeated three times using the bound-wire method.

## 2.13 Gait behavior score

This study assessed rats for their gait behavior 24 hours after administering sodium urate crystals. A scoring system, ranging from 0 to 3, was implemented to evaluate the severity of their gait impairment. A score of 0 denoted a normal gait, while a score of 3 indicated severe claudication. A score of 1 reflected normal claudication with slightly bent limbs at the injection site, whereas a score of 2 represented moderate claudication where the limb touched the ground.

## 2.14 Determination of IL-1β and TNF-α in rat synovial tissue by ELISA

All rats were euthanized after seven days of gavage administration. The fur was removed by placing the rats in an ice bath, and subsequently, the tissues were ground with liquid nitrogen and saline using a tissue homogenizer. The resulting mixture was centrifuged at 4℃ and 3000 rpm for 10 minutes. Subsequently, the supernatant was stored at -80℃. The levels of inflammatory factors IL-1β and TNF-α were measured using ELISA kits following the manufacturer's instructions.

## 2.15 Hematoxylin-eosin (HE) staining of rat ankle joint tissues

The freshly collected ankle tissues were fixed in a 4% formalin solution for 24 hours before being placed into an embedding box. Once in the box, the tissues were trimmed and rinsed with water to remove any remaining fixatives. Subsequently, the tissues were dehydrated overnight in a dehydrator. After dehydration, the tissues were embedded in paraffin and sectioned. Hematoxylin and eosin (HE) staining was performed: the paraffin sections were first subjected to xylene dewaxing for 5 minutes, followed by two additional 5-minute xylene dewaxing steps. Subsequently, the sections were treated with anhydrous ethanol for 1 minute, followed by 30 seconds in anhydrous ethanol, 95% ethanol, 85% ethanol, and 75% ethanol, respectively. The sections were then rinsed with tap water for 30 seconds and stained with hematoxylin for 10 minutes. After rinsing them again in tap water for 30 seconds, the sections were briefly treated with 1% hydrochloric acid and 0.5% ammonia anti-blue solution. Following a minute-long tap water rinse, the sections were exposed to eosin aqueous solution for 2 minutes, followed by a 30-second tap water rinse. Dehydration was achieved by treating the sections with 85% ethanol for 10 seconds, then 95% ethanol for 10 seconds, and finally, two rounds of dehydration with anhydrous ethanol for 30 seconds each. The sections were then rendered transparent by immersing them in xylene three times, each for a minute. Once transparent, the sections were dried in a 37.5℃ oven. To preserve the

sections, the film was sealed with neutral resin, and only after the resin had completely dried were the sections ready for observation and photography under a microscope.

# 2.16 LC-MS/MS

## 2.16.1 Sample processing

To prepare the sample for analysis, 50 mg of Xiaoxianggou ethyl acetate effective part lyophilized powder was weighed and dissolved in 400 µL of cold methanol, along with the internal standard. The solution was vortexed and shaken for 2 minutes. Subsequently, the sample was ground using two steel balls at a frequency of 50 Hz for 4 minutes at 4 ℃. After grinding, the steel balls were removed, and the sample was thoroughly extracted using an ultrasonic probe for 30 minutes. Following extraction, the sample was vortexed for an additional 2 minutes and then kept at a low temperature for 10 minutes. The samples were centrifuged at 14000 rpm for 15 minutes at 4 ℃. Following centrifugation, 200 µL of the supernatant was transferred to a new EP tube, concentrated through centrifugation, and stored in a refrigerator at -20 ℃. Prior to the analysis, the centrifuged extracts were re-dissolved in 100 µL of a 20% methanol/water solution. The solution was thoroughly shaken until complete dissolution, and then the supernatant was subjected to centrifugation for positive and negative ion mode analysis.

## 2.16.2 Chromatographic conditions

Positive ion mode: The BEH C8 column (1.7 µm, 2.1×100 mm) from Waters, USA, was used. The mobile phase consisted of water for phase A and acetonitrile for phase B. The column temperature was 50 ℃, and the flow rate was 0.35 mL/min. The elution conditions were as follows: 0–1 min, 5% B; 1-27.5 min, 100% B; 27.5–30 min, 5% B.

Negative ion mode: The HSS T3 column (1.8 µm, 2.1×100 mm) from Waters, USA, was employed. The mobile phase included water for Phase A and 95% methanol for Phase B. The column temperature was maintained at 50 ℃, and the flow rate was set at 0.35 mL/min. The elution conditions were as follows: 0–1 min, 5% B; 1–22 min, 100% B; 22–25 min, 5% B.

## 2.16.3 Mass spectrometry conditions

Positive ion mode: HESI-Positive mode with heated electrospray ion source + primary full scan + DDA secondary sub-ion scan mode. Aux gas heater temperature (°C): 350; sheath gas flow rate (Arb): 35; aux auxiliary gas flow rate (Arb): 8. S-lens RF level: 50; massmass range (m/z): 70-1050, Full ms resolution: 70000; MS/MS resolution: 17500resolution: 17500; TopN: 5; NCE/stepped NCE: 20,40NCE: 20,40.

Negative ion mode: HESI-Negative mode with a heated electrospray ion source, using a first-stage full scan + DDA second-stage sub-ion scan mode. 350; Sheath gas flow rate (Arb): 35; Aux gas flow rate (Arb): 8; S-lens RF level: 50; Mass range (m/z): 70-1050, Full ms resolution: 70000; MS/MS resolution:17500; TopN: 5; NCE/stepped NCE: 20,40.

# 2.17 Active ingredient and target screening

The mass spectrometry data of the effective part of Xiaoxianggou ethyl acetate were analyzed and compared with the TCMSP database platform (https://old.tcmsp-e.com/tcmsp.php) to identify the major chemical components. The main active ingredients with potential therapeutic effects were selected based on drug-like properties (> 0.18) and oral bioavailability (> 30%). The identified active ingredients were then searched in the compound database PubChem (https://pubchem.ncbi.nlm.nih.gov/) to obtain their 2D structures. These structures were subsequently imported into the Swiss Target Prediction database (http://swisstargetprediction.ch/) to identify potential drug targets. The target prediction was performed using "homo sapiens" as the selected species.

# 2.18 Acquisition of gout targets

To identify disease targets for gout arthritis, we searched OMIM data (https://omim.org/), GeneCards database (https://www.genecards.org/), DisGeNet database (https://www.genecards.org/), CTD database (https://www.genecards.org/), GeneBank database(https://www.genecards.org/), DisGeNet database (https://www.disgenet.org/), CTD database (https://ctdbase.org/), and GeneBank database (https://www.ncbi.nlm.nih.gov/genbank/) using the keyword "gout arthritis". Targets were considered relevant if they had a correlation score of 1 or higher in GeneCards and a score of 0.2 or higher in DisGeNet. Following the search, the identified targets were merged and duplicate entries were eliminated

# 2.19 Construction of PPI network and acquisition of key targets

To determine the potential targets of Xiaoxianggou ethyl acetate, an effective treatment for GA, we analyzed the candidate targets for each active ingredient using the Sento Academic online tool (https://www.xiantao.love/products). These targets were intersected with the targets for gout. The resulting network of common target gene protein interactions was constructed using the String database (https://string-db.org/), where a minimum interaction score of medium confidence 0.400 was required. To enhance clarity, unconnected nodes were eliminated from the network. The constructed protein-protein interaction (PPI) network was exported in TSV format and visualized using Cytoscape v3.9.1. In Cytoscape 3.9.1, the cytoHubba plugin was utilized to screen for core targets based on their maximal clique centrality (MCC) scores. The MCC score indicates a gene's importance in the network, with higher scores indicating greater significance.

# 2.20 GO function and KEGG analysis

We conducted Gene Ontology (GO) and Kyoto Encyclopedia of Genes and Genomes (KEGG) analyses on the target genes in the protein-protein interaction (PPI) network using R 4.1.3. We identified the top 10 biological processes (BP), cellular components (CC), molecular functions (MF), and signaling pathways using $P < 0.05$ and $Q < 0.05$ as significance criteria. The obtained results were then visually represented using bar graphs.

# 2.21 Molecular docking

The key-acting protein genes were obtained from the UniProt database (https://www.uniprot.org/), and their protein pdb files were downloaded from the PDB database (http://www.rcsb.org/). The PyMOL software removed small molecule ligands and water molecules from the target proteins. AutoDockTools-1.5.6 was then employed to dock potential active ingredients of the small aromatic hook with the key-acting protein molecules. The quality of docking was assessed based on the binding energy, with a binding energy < -5.0 kJ/mol indicating good binding and <-7.0 kJ/mol indicating binding solid activity to the core target protein [27, 28]. The interactions between each potential active component of chamomile and the key acting target proteins were visualized and displayed as 3D maps using PyMOL software.

## 2.22 Statistical analysis

Statistical analysis was performed using SPSS 26.0, and GraphPad Prism 8.0.2 was used to generate charts. The data was expressed as mean ± standard deviation (SD). Normality tests were performed using the Shapiro-Wilk test, while chi-square tests were employed to analyze differences among data groups. One-way analysis of variance (ANOVA) was utilized to compare differences between data groups, and for two-way comparisons, either the LSD test (for chi-square) or the Games-Howell test (for chi-square) was employed. Statistical significance was considered at $P < 0.05$.

# 3 Results

## 3.1 Optimization of the extraction process and analysis of the total phenolic content of Xiaoxianggou

Single-factor experiments were conducted to investigate the effects of extraction time, material-to-liquid ratio, ethanol content, extraction temperature, and number of extractions on the total phenolic content of Xiaoxianggou. Our findings revealed that the extraction time and material-liquid ratio had minimal effects on the total phenol yield of Xiaoxianggou. However, the extraction temperature and volume fraction of ethanol impacted the total phenol yield. The optimal extraction temperature was approximately 70 ℃, and the highest extraction rate was achieved when the ethanol content was around 70%. Notably, after two extractions, the total phenol content of Xiaoxianggou was completely extracted (Fig. 1A).

An orthogonal test was conducted to analyze the impact of three factors on total phenol yield. The results of the range analysis revealed that R(B) > R(A) > R(C) (Table 3). Additionally, the study found that the ethanol volume fraction (B) had the greatest effect on the extraction rate in Xiaoxianggou, followed by temperature (A) and material-to-liquid ratio (C). Utilizing the results from the single-factor experiments, the optimal conditions for extracting total phenols from Xiaoxianggou were determined to be $A_2B_1C_2$. These conditions included an extraction temperature of 70 ℃, an ethanol volume fraction of 60%, and a material-liquid ratio of 1:30. To validate the optimal process, three additional experiments were conducted, and the average yield of total phenol from Xiaoxianggou was found to be 1.43%. The variance analy analysis indicated that the three factors examined did not significantly impact the extraction rate of total phenols in Xiaoxianggou (Table 4).

The total phenolic content of each phase of Xiaoxianggou was assessed individually. The findings indicate that the extracts of Xiaoxianggou exhibited the following order in terms of total phenolic content: ethyl acetate phase > n-butanol phase > aqueous phase. Specifically, the ethyl acetate phase exhibited significantly higher levels of total phenolic content than the n-butanol and aqueous phases (Fig. 1B).

Table 3
Ultrasound-assisted L9 ($3^3$) orthogonal experimental design for extracting total phenols from Xiaoxianggou.

| Groups | A | B | C | Total phenolic content |
|---|---|---|---|---|
| 1 | 1 | 1 | 1 | 1.3200 |
| 2 | 1 | 2 | 3 | 1.0970 |
| 3 | 1 | 3 | 2 | 1.2079 |
| 4 | 2 | 1 | 3 | 1.3757 |
| 5 | 2 | 2 | 2 | 1.3534 |
| 6 | 2 | 3 | 1 | 1.1879 |
| 7 | 3 | 1 | 2 | 1.2976 |
| 8 | 3 | 2 | 1 | 1.2790 |
| 9 | 3 | 3 | 3 | 1.2106 |
| *k*1 | 3.62 | 3.99 | 3.79 | |
| *k*2 | 3.92 | 3.73 | 3.86 | |
| *k*3 | 3.79 | 3.61 | 3.68 | |
| *K*1 | 1.21 | 1.33 | 1.26 | |
| *K*2 | 1.31 | 1.24 | 1.29 | |
| *K*3 | 1.26 | 1.2 | 1.23 | |
| *R* | 0.1 | 0.13 | 0.06 | |

Table 4
Analysis of variance

| Factor | DEVSQ | Df | F | F critical value | P |
|---|---|---|---|---|---|
| A | 0.014 | 2 | 0.007 | 0.757 | > 0.05 |
| B | 0.026 | 2 | 0.013 | 1.381 | > 0.05 |
| C | 0.005 | 2 | 0.003 | 0.275 | > 0.05 |
| Error | 0.019 | 2 | | | |

# 3.2 Cytological screening of the effective parts of the Xiaoxianggou

The RAW264.7 cells were treated with extracts of Xiaoxianggou at each extraction site for 24 hours. The cell viability was assessed using the MTS method. The results revealed that the cell viability of RAW264.7 cells remained unaffected by the ethyl acetate and n-butanol phases at concentrations below 40 μg/mL, as well as the aqueous phase at concentrations below 400 μg/mL when compared to the control group. Henceforth, the ethyl acetate and n-butanol phases at concentrations of 10, 20, and 40 μg/mL (Fig. 2A, B), and the aqueous phase at concentrations of 100, 200, and 400 μg/mL (Fig. 2C) were selected for further experiments.

RAW264.7 cells were treated with MSU crystals for 24 hours, and the expression level of TNF-α was measured using ELISA. The results showed a significant increase in TNF-α expression levels in all groups treated with 100–600 μg/mL of MSU compared to the control group ($P < 0.001$). To avoid the effects of high concentrations of MSU on cell viability, a concentration of 400 mg/L MSU crystals was chosen to induce inflammation in macrophages for 24 hours (Fig. 2D).

Based on successful modeling, we treated the RAW264.7 cells with each extracted part of Xiaoxianggou for 6 hours and measured the expression level of TNF-α. Our results showed that the TNF-α level was significantly higher in the Model group compared to the control group ($P < 0.01$), indicating successful modeling. The study indicated that the ethyl acetate phase of Xiaoxianggou at concentrations of 10, 20, and 40 μg/mL exhibited the ability to reduce the production of TNF-α by MSU-induced RAW264.7 macrophages (Fig. 2D), with the most significant reduction at 40 μg/mL ($P < 0.01$). However, the concentrations of each of the aqueous and n-butanol phases of Xiaoxianggou promoted the expression of TNF-α in macrophages (Fig. 2F, G) ($P < 0.0001$). Based on the observed inhibitory effect of Xiaoxianggou ethyl acetate on the elevated levels of inflammatory factors induced by MSU, it is suggested that it could be a potential target for the treatment of gouty arthritis. Further focused study on this aspect is proposed for future research.

# 3.3 Therapeutic effect of Xiaoxianggou ethyl acetate active part on GA rats

Except for the control group, all rats were injected with MSU crystals at the ankle joint, and the degree of ankle swelling and gait behavior of rats were measured. The results demonstrated that the Model group exhibited a significant increase in foot swelling six hours after injecting sodium urate crystals. The foot swelling peaked 12 hours later and persisted for 48 hours post-injection. Compared to the Model group, administering Xiaoxianggou ethyl acetate effective part at a dosage of 12.5 g/(kg·d) reduced the degree of foot swelling at the 24-hour mark following the induction of sodium urate crystals (Table 5). Furthermore, this treatment significantly mitigated the gait score of the rats 24 hours after the sodium urate crystal injection (Table 6). Both colchicine and Xiaoxianggou ethyl acetate effectively part demonstrated the ability to reduce the gait scores of rats with gouty arthritis, with the high-dose group exhibiting a more pronounced effect.

ELISA was used to detect the expression of TNF-α and IL-1β in the ankle joint tissues of rats in each group. The findings demonstrated a notable increase in both IL-1β and TNF-α expression in the arthritic tissues of rats from the Model group following the administration of sodium urate for 48 hours. The medium dose administration group significantly reduced the expression of IL-1β in the arthritic tissues of rats (Fig. 3A), whereas all dosing groups (low, medium, and high) exhibited a reduction in TNF-α expression in the arthritic tissues of rats (Fig. 3B).

The ankle joint tissues of rats were analyzed using HE staining to observe pathological changes. The findings revealed that the ankle joint tissues of rats in the control group displayed a smooth surface, with synovial tissue cells distributed uniformly and no presence of inflammatory cells. In contrast, the experimental group exhibited a distinct inflammation response, characterized by disorganized synovial tissue and a substantial infiltration of inflammatory cells. However, both the colchicine and medium-high dose administration groups demonstrated a reduction in inflammatory cell infiltration, as well as an improvement in the congestion and edema of the surrounding soft tissues. These findings suggest that the ethyl acetate phase of Xiaoxianggou has the potential to ameliorate synovial hyperplasia and inflammatory cell infiltration in GA rats (Fig. 3C).

Table 5
Xiaoxianggou ethyl acetate effective part reduced paw swelling in rats with gouty arthritis

| Group | Dosage(g/kg·d) | Rat ankle joint circumference(cm) | | | | |
|---|---|---|---|---|---|---|
| | | 0h | 6h | 12h | 24h | 48h |
| Control | — | 2.08 ± 0.12 | 2.21 ± 0.10 | 2.24 ± 0.07 | 2.14 ± 0.11 | 2.08 ± 0.15 |
| Model | — | 2.06 ± 0.05 | 2.73 ± 0.12* | 2.98 ± 0.19* | 2.83 ± 0.14* | 2.56 ± 0.13* |
| Colchicine | 0.0003 | 2.08 ± 0.07 | 2.86 ± 0.21 | 2.95 ± 0.11 | 2.76 ± 0.17 | 2.48 ± 0.16 |
| L-FPH-E | 3.125 | 2.08 ± 0.05 | 2.80 ± 0.16 | 2.96 ± 0.21 | 2.75 ± 0.16 | 2.43 ± 0.18 |
| M-FPH-E | 6.25 | 2.04 ± 0.05 | 2.71 ± 0.18 | 2.91 ± 0.15 | 2.71 ± 0.15 | 2.54 ± 0.23 |
| H-FPH-E | 12.5 | 2.05 ± 0.08 | 2.85 ± 0.12 | 2.81 ± 0.11# | 2.64 ± 0.12# | 2.48 ± 0.24 |

L-FPH: Low-dose group of Xiaoxianggou ethyl acetate phase; M-FPH: Medium-dose group of Xiaoxianggou ethyl acetate phase; H-FPH: High-dose group of Xiaoxianggou ethyl acetate phase; Compared to control group,*$P$< 0.05. Compared with model group, #$P$< 0.05.( $X$ ± s, n = 8)

Table 6
Xiaoxianggou ethyl acetate effective part reduced gait score in rats with gouty arthritis

| Group | Dosage(g/kg·d) | Gait score |
|---|---|---|
| Control | — | 0.00 ± 0.00 |
| Model | — | 2.50 ± 0.53 |
| Colchicine | 0.0003 | 2.38 ± 0.52 |
| L-FPH-E | 3.125 | 2.25 ± 0.46 |
| M-FPH-E | 6.25 | 2.25 ± 0.46 |
| H-FPH-E | 12.5 | 1.88 ± 0.64* |

Compared with model group, *$P$< 0.05.(—$X$±s, n=8)

# 3.4 Identification of potential active ingredients in the Xiaoxianggou ethyl acetate effective parts by LC-MS/MS

The active component of Xiaoxianggou ethyl acetate effective parts was analyzed using HPLC-MS/MS in both positive and negative ESI ionization modes. The analysis produced a total ion flow diagram (Fig. 4A, B), and 95 chemical components were identified by comparing them with literature and controls. Among these components, the top 25% with the highest relative content were selected as candidate markers, including flavonoids, flavanols, biflavonoids, terpene lactones, organic acids, and other compounds. Through a screening process utilizing the TCMSP database, a total of 14 compounds were identified (Table 7)

Table 7
Identification of the potential components of lyophilized powder at the Xiaoxianggou ethyl acetate effective part.

| No. | RT/min | m/z | compound | CAS | Ion Form |
|---|---|---|---|---|---|
| 1 | 4.25 | 290.29 | catechin | | +/- |
| 2 | 3.00 | 290.29 | epicatechin | 35323-91-2 | + |
| 3 | 8.78 | 271.26 | pelargonidin | | + |
| 4 | 6.50 | 286.25 | auresudidin | 5281220 | + |
| 5 | 3.21 | 302.25 | quercetin | | + |
| 6 | 6.48 | 304.27 | 5,2'-dihydroxyflavone | 78708-33-5 | + |
| 7 | 7.76 | 288.27 | eriodictyol | 552-58-9 | - |
| 8 | 4.98 | 304.27 | taxifolin | 480-18-2 | - |
| 9 | 9.54 | 286.25 | luteolin | 491-70-3 | - |
| 10 | 9.85 | 286.25 | kaempferol | 520-18-3 | - |
| 11 | 6.02 | 270.25 | lucidin | | + |
| 12 | 14.04 | 246.28 | marmesin | | + |
| 13 | 5.10 | 302.3 | hesperetin | | + |
| 14 | 2.78 | 302.25 | 6-hydroxyluteolin 7-glucoside | | - |

# 3.5 Network pharmacology and mechanism validation

The Xiaoxianggou ethyl acetate extract was analyzed to determine its active constituents, utilizing 2D structures sourced from the PubChem database. The Swiss Target Prediction database was then searched to identify the target genes of these active ingredients. Following sorting and adjustment for Probability value, a total of 198 drug targets associated with the active ingredients were identified. The resulting drug targets were then intersected with 417 GA targets using Venn diagram analysis, yielding 47

potential targets for the active ingredients of Xiaoxianggou ethyl acetate extract in the treatment of GA (Fig. 5A).

The String database was utilized to explore the interaction between potential targets of chamomile's active ingredients for GA treatment. The network consisted of 47 nodes with an expected edge value of 46. Surprisingly, the edge value was significantly higher at 182, indicating a highly interconnected network. The network's significance was evident, with an average node degree of 7.74 and a PPI enrichment value of $P < 1.0e-16$. Following removing unconnected nodes, the target relationships were ranked based on their degree values using cytoscape software. Notably, the analysis highlighted VEGF-α, MMP9, TLR-4, PTGS2, SRC, and PPARG as having prominent degrees within the network (Fig. 5B, C).

GO functional enrichment analysis used a $padj < 0.05$ threshold for significant enrichment. The analysis yielded 2255 biological processes focused primarily on regulating inflammatory response, producing immune response cytokines, metabolism of reactive oxygen species, and lymphocyte activation of the immune response. Additionally, 79 entries related to cell composition were identified, such as inflammatory vesicle complex, intranuclear membrane, cytoplasmic vesicles, membrane rafts, and membrane microregions. The molecular functions related to 149 entries primarily included cytokine receptor binding, growth factor receptor binding, DNA-binding transcription factors, cytokine activity, nuclear hormone receptor binding, and signaling receptor activator activity (Fig. 5D). KEGG pathway enrichment analysis identified a total of 152 signaling pathways, with the top 10 pathways including Th17 cell differentiation, NOD-like receptor signaling pathway, Toll-like receptor signaling pathway, PI3K/Akt signaling pathway, FoxO signaling pathway, rheumatoid arthritis, and NF-κB signaling pathway, among others (Fig. 5E). Based on the literature and pathway enrichment analysis results, the TLR-4/MyD88 signaling pathway was selected for further investigation.

The molecular docking validation of each potential active ingredient of Xiaoxianggou with TLR-4 target protein was calculated using AutoDockTools. The results revealed that the binding energy of each active ingredient was less than − 5.0 kJ/mol, indicating good binding ability with TLR-4 target protein (Table 8). Quercetin, eriodictyol and 5,2'-dihydroxyflavone showed strong binding activity with TLR-4. The docking results were visualized in PyMOL software, suggesting that the ethyl acetate active site of Xiaoxianggou may treat GA by acting on the above TLR-4 targets. The molecular docking results of each potential active ingredient of Xiaoxianggou with TLR-4 target proteins are presented below (Fig. 5F).

Figure 5 Venn diagram of the intersection of each active ingredient of Xiaoxianggou ethyl acetate effective part with GA gene (A). Protein interaction network diagram (B) and drug target modulation network (C) of Xiaoxianggou ethyl acetate effective part for GA treatment. GO functional was performed on the screened 47 target genes highly related to GA (D). The figure shows the top 10 GO terms in biological regulation (BP, green), cellular component (CC, orange), and molecular function (MF, purple) respectively. KEGG enrichment analysis of the signaling pathways that the differently expressed genes may be involved in, the size of the dots indicates the number of differential genes annotated to the

pathway, and the color indicates the adjusted P value (E). Molecular docking pattern of Xiaoxianggou potential active component to TLR-4 target proteins (F).

Table 8 Molecular docking of Xiaoxianggou potential active component to TLR-4 target proteins.

| compound | TLR-4 | |
|---|---|---|
| | free energy (KJ/mol) | hydrogen bonds |
| catechin | -8.2 | 4 |
| epicatechin | -8.0 | 4 |
| pelargonidin | -8.5 | 3 |
| auresudidin | -8.5 | 6 |
| quercetin | -9.0 | 4 |
| 5,2'-dihydroxyflavone | -9.4 | 5 |
| eriodictyol | -9.0 | 5 |
| taxifolin | -7.7 | 5 |
| luteolin | -8.7 | 5 |
| kaempferol | -8.7 | 1 |
| lucidin | -8.8 | 1 |
| marmesin | -8.0 | 3 |
| hesperetin | -8.2 | 2 |
| 6-hydroxyluteolin 7-glucoside | -8.6 | 5 |

### 3.6 Reduction of TLR4/MYD88 pathway-related gene mRNA expression by the Xiaoxianggou ethyl acetate effective part

To investigate the potential mechanisms of Xiaoxianggou ethyl acetate's efficacy in treating GA, we conducted an experiment using various concentrations of Xiaoxianggou ethyl acetate (10, 20, 40 μg/mL) to intervene with macrophages for 6 hours. Subsequently, 400 μg/mL MSU was added for 24 hours. We then employed qRT-PCR to analyze the mRNA expression of *TLR4, MYD88, NF-κB, TNF-α*, and *IL-1β* in the macrophages. The results revealed a significant increase in the mRNA expression of *MYD88, NF-κB, TNF-α*, and *IL-1β* in the Model group. However, a significant reduction in the expression levels of each gene was observed in the middle and high-dose groups, particularly in the high-dose group, compared to the Model group. These findings suggest that Xiaoxianggou ethyl acetate may act on the TLR4/MYD88 pathway for GA treatment (Fig. 6).

## 4. Discussion

The pathogenesis of GA remains unclear, and the existing pharmaceutical treatments are associated with significant adverse effects. Traditional Chinese medicine, specifically ethnic medicine, has been extensively investigated for its potential in treating gouty arthritis and has shown notable benefits [30–33]. Studies have revealed the effectiveness of Xiaoxianggou, a herbal medicine, in the treatment of GA. However, there is limited available information regarding its pharmacological mechanism of action and the specific components responsible for its efficacy [24].

Polyphenolic compounds, rich in hydroxyl groups, demonstrate various biological activities, such as antioxidant, anti-inflammatory, and antibacterial properties [34]. Previous research has indicated that Xiaoxianggou is a rich source of catechins, chlorogenic acid, vanillic acid and other polyphenols [6]. Therefore, in this study, the total phenolic content was utilized as the extraction quality control standard to optimize the extraction process of Xiaoxianggou.

Chinese medicine contains a wide range of compounds with similar chemical properties that confer therapeutic effects. The efficacy of herbal medicines relies on the synergistic action of multiple components or active constituents [35]. One common approach to extracting these active fractions involves using different polar solvents. LYU et al. experimented with the extract of Xiaoxianggou using various polar solvents [36]. The researchers evaluated the inhibition rate of Xanthine oxidase and identified the n-butanol extraction phase as the effective treatment component. Preliminary pre-experiments were conducted in this study to select ethyl acetate, n-butanol, and water as extractants to prepare potential effective fractions for further investigation. The results showed that ethyl acetate extracts (10, 20, and 40 μg/mL) from Xiaoxianggou effectively suppressed the MSU-induced increase in inflammatory factor levels dose-dependently during drug cytotoxicity screening. In contrast, the n-butanol extract and aqueous extract of Xiaoxianggou exhibited increased TNF-α expression. This peculiar observation could be attributed to various factors, including the higher polarity of n-butanol, which may result in solvent residue in the extract, leading to a false positive effect. Moreover, the extraction process might have unintentionally extracted non-active components and the relevant preparation process may have had some imperfections.

Ultrasonic-assisted extraction technology is frequently employed for the extraction of traditional Chinese medicine. This approach employs the energy generated by ultrasonic waves in the solvent to induce thermal and mechanical effects, ultimately resulting in effective extraction by breaking down cell walls [37]. This method provides numerous benefits, such as a short extraction time, high efficiency, and cost-effectiveness [38]. In this study, we optimized and validated the ultrasonic extraction process of Xiaoxianggou's total phenols using single-factor experiments and orthogonal experimental design.

The study found that extraction times were determined based on time considerations and economic cost. Interestingly, the duration of extraction had minimal influence on the overall yield of phenol. Certain references indicate that prolonging the extraction time could result in more dissolved impurities [39]. Therefore, we opted to set the extraction time at 30 minutes. On the other hand, the material-liquid ratio,

extraction temperature, and ethanol volume fraction significantly affected the total phenol yield. We conducted orthogonal experiments concerning these three factors to optimize the extraction process. After optimizing the extraction process, the extraction rate of total phenol was 1.43%, which was higher than the experimental results in the orthogonal design table, indicating that the extraction process is more stable and can serve as a viable technique for the ultrasonic extraction of phenol from Xiaoxianggou.

The development of GA is a complex process, where the deposition of MSU crystals in the joints and surrounding soft tissues is widely recognized as a significant contributing factor [40]. When immune cells such as macrophages and neutrophils encounter MSU crystals at the affected site, they release inflammatory factors, such as IL-1β and TNF-α, triggering a cascade of inflammatory reactions and joint damage [41]. Emira Bousoik et al. established a gout model in vitro using 100 μg/mL MSU crystal to intervene with macrophages. The activity of Lactate dehydrogenase and the expression level of IL-1β in the supernatant of macrophages was detected [42]. The initial experimental findings indicate that the IL-1β inflammatory factor cannot be identified in the macrophage supernatant. This observation could be attributed to the absence of the Asc gene in macrophages, resulting in the loss of assembly function of the NLRP3 inflammatory complex [43, 44]. Consequently, the precursor IL-1β cannot undergo further cleavage to form mature bodies. Feng Jia et al. have demonstrated that the intervention of different concentrations of MSU crystals in RAW264.7 macrophages for 24 hours resulted in significant differences in the expression of inflammatory factors compared to the blank control group [45, 46]. Therefore, in this study, we aimed to establish a gout cell model by stimulating mouse RAW264.7 macrophages with various concentrations of MSU crystals for 24 hours. The success of modeling was evaluated by measuring the expression of TNF-α in the supernatant using ELISA. The study found a significant difference between the group treated with 400 μg/mL MSU and the control group ($P < 0.0001$). However, even though the expression of TNF-α was higher in the group treated with 600 μg/mL MSU, we chose to use 400 μg/mL MSU crystals to establish the inflammation model in macrophages for 24 hours. This decision was made due to concerns that using a higher MSU concentration could compromise cell viability and morphology.

The Coderre puncture method is a traditional animal model for GA. In this method, joint inflammation is induced by injecting monosodium urate (MSU) suspension into the joint cavity of rats [47]. However, this method has limitations, such as mechanical damage and fluid leakage in rat joints due to the narrow joint space. To overcome these disadvantages, researchers have discovered an effective improvement: injecting a volume of no more than 100 μL along the posterior Achilles tendon edge of the rat ankle at a 30–40° angle to the axis of the lower leg [48, 49]. Huang Huogao et al. discovered that injecting 20–25 mg/mL MSU into a single ankle joint of rats accurately reflected the pathophysiological processes of GA [50, 51]. These GA models remained stable for up to one week after preparation. In our study, to create an acute GA model, we injected 100 μL of 25 mg/mL MSU solution into the joint cavity by downwardly puncturing the medial aspect of the posterior Achilles tendon of the rat ankle at a 30°-40° angle. The results showed a significant increase in the gait behavior score of rats 24 hours after crystal injection, along with significant ankle joint swelling. HE staining revealed a strong inflammatory response in the

affected joint, characterized by disordered synovial tissue structure and a high level of inflammatory cell infiltration. Furthermore, the levels of TNF-α and IL-1β in the joint tissue were significantly increased ($P < 0.0001$). Administration of colchicine resulted in a decrease in ankle circumference and gait behavior scores compared to the model group, although the difference was not statistically significant, potentially due to the low dosage of administration. Conversely, intervention with the ethyl acetate effective part of Xiaoxianggou significantly reduced ankle swelling and joint pathological damage in rats with gouty arthritis. Moreover, the expression of TNF-α and IL-1β in joint tissues significantly decreased ($P < 0.001$), indicating the pharmacological effect of the ethyl acetate effective part of Xiaoxianggou in inhibiting GA.

Chinese herbal medicines are known for their complexity, as the same herb can exhibit varying components and contents depending on factors such as origin, climate, temperature, humidity, and harvesting time. Therefore, it is crucial to identify and analyze the components of Chinese herbal medicines. The liquid-liquid mass spectrometry technique is effective for qualitative and quantitative analysis of these components. This technique allows for thoroughly identifying all components, making it particularly suitable for investigating unknown components present in Chinese herbal medicines. Due to its effectiveness, this technique has gained wide application within the metabolomics of Chinese herbal medicines. In this study, we employed the LC-MS/MS technique to quantify fourteen potential active components within the ethyl acetate effective part of Xiaoxianggou. Among these components were catechin, quercetin, and kaempferol, with polyphenols being the most significant. We analyzed the relevant active ingredients by utilizing PubChem and other online databases. Notably, we discovered that TH17 cell differentiation, Toll-like receptor signaling pathway, and NOD-like receptor signaling pathway are closely associated with the therapeutic effects of Xiaoxianggou ethyl acetate effective part in the treatment of gouty arthritis.

Toll-like receptors, specifically TLR4, TLR2, and the bridging protein MYD88 are crucial pattern recognition receptors in the immune system that contribute to the development of inflammation. Among the various signaling pathways investigated in the pathogenesis of GA, the TLR4/MYD88 pathway has been extensively studied. TLR4 acts as a pivotal pattern recognition receptor, effectively detecting pathogen-associated molecular patterns (PAMPs). Upon stimulation by MSU, TLR4 cooperates with MYD88 to activate the transcription factor NF-κB. Consequently, this triggers the transcription and expression of inflammatory factors such as IL-1β, leading to the initiation of an inflammatory cascade reaction [52]. In this study, we conducted qRT-PCR to detect the expression levels of TLR4, MYD88, NF-κB, TNF-α, and IL-1β, molecules involved in the TLR4/MYD88 signaling pathway. Our findings demonstrate that the ethyl acetate effective part of Xiaoxianggou may exert anti-inflammatory effects by regulating the TLR4/MYD88 pathway, resulting in reduced production and release of inflammatory factors.

Research has demonstrated that Macrophage polarization is crucial in developing gouty arthritis [53]. This process can be categorized into two stages: M1 and M2, each characterized by specific markers [54]. M1 polarization is marked by the presence of IFN-γ, IL-1β, TNF-α, and INOS, whereas M2 polarization is characterized by the expression of markers such as IL-10 and Arg-1, among others [55]. Studies have indicated an increase in M1 macrophages at the lesion site in rats with gouty arthritis. However, it has

been found that the activation of sirt1 can inhibit the tendency of M1 polarization in rats and ameliorate MSU-induced inflammation [56].

In this study, the expression of TNF-α significantly increased in macrophage supernatants after a 24-hour intervention with MSU ($P < 0.0001$). All the concentration groups of the ethyl acetate effective part of Xiaoxianggou observed a varying degree of reduction in TNF-α expression. These findings suggest that MSU induces M1-type polarization in macrophages, and the ethyl acetate effective part of Xiaoxianggou may inhibit M1-type macrophage polarization, thereby providing anti-GA effects. However, it is important to note that this study solely focused on measuring the detection index of M1-type macrophage polarization markers without examining associated markers of M2-type macrophage polarization. Hence, further research is necessary to determine if the ethyl acetate effective part of Xiaoxianggou can effectively treat GA by promoting the transition of M1-type macrophages to M2-type macrophages.

This study discovered that the effective component of ethyl acetate in Xiaoxianggou could effectively reduce macrophage inflammation and gouty arthritis caused by MSU crystals in rats. The mechanism underlying this effect is probably associated with inhibiting the TLR4/MYD88 signaling pathway. It is hypothesized that the anti-gouty arthritis effect of Xiaoxianggou may be attributed to macrophage polarization, but additional research is required to validate this assumption. Overall, this research lays the groundwork for the potential use of Xiaoxianggou as a treatment for gout and other related conditions.

# 5. Conclusions

The optimum extraction process for Xiaoxianggou was determined by assessing the total phenol content as the quality control standard. This process includes an extraction temperature of 70℃, a 60% volume fraction of ethanol, and a solid-liquid ratio of 1:30. The ethyl acetate phase of Xiaoxianggou has been found to decrease TNF-α levels in macrophages in the RAW264.7 inflammatory model. Moreover, it has been observed to enhance the inflammatory performance in the GA rat model, suggesting its potential as an effective active ingredient in Xiaoxianggou. The ethyl acetate component of Xiaoxianggou has demonstrated significant efficacy in the treatment of GA, with the Tlr4/myd88 signaling pathway playing a pivotal role in this process.

# Declarations

### Author Contributions

Yulong Huang and Xiaohui Lin contributed equally to this work. Yulong Huang and Xiaohui Lin played pivotal roles in the conceptualization and design of the study, with Minhua Lin contributing significantly to data collection and analysis. Reheman Aikebaier and Yujia Wang were instrumental in the development and execution of the methodology, while Di Zhong and Bingying Xiao focused on software and validation tasks, ensuring the reliability of the tools and methods used. Jiangyuan Zhang, Lingling Zhang, and Zichun Chen offered substantial expertise in the interpretation of data, enriching the study's

findings with their insightful analyses. Xuekun Nie, meanwhile, was responsible for the overall project administration and supervision, guiding the project towards its successful completion. Collectively, their diverse contributions were essential in advancing the research objectives, demonstrating a commendable synergy in their collaborative efforts.


### Funding

This work was supported by the Natural Science Foundation of Fujian Province (2022J011220), the Natural Science Foundation of Fujian Province (2023J011082) and Special Research Project of Ningde Normal University Affiliated Hospital (2022Y1002).


### Declaration of competing interest

We confirm that there are no conflicts of interest associated with this publication.

# References


1. WANG W, MAO J, YU H, et al. Study on quality standard of traditional She medicine Xiaoxianggou [J]. Chinese Archives of Traditional Chinese Medicine, 2015, 33(08): 1979-81 + 2075.
2. Zhejiang Provincial Food and Drug Administration. Zhejiang provincial standards of processing chinese crud drugs [J]. Beijing: The Medicine Science and Technology Press of China, 2015:13–14.
3. FENG H, DAI H, BAI S et al. Protective effect of Ficus pandurata extract on alcohol-induced acute liver injury base on pyroptosis [J]. Chinese Journal of Experimental Traditional Medical Formulae, 2020, 26(13): 125–31.
4. LV H, ZHANG X, CHEN X, et al. Phytochemical compositions and antioxidant and anti-inflammatory activities of crude extracts from Ficus pandurata H. (Moraceae) [J]. Evid Based Complement Alternat Med, 2013, 2013: 215036.
5. NIE W, ZHANG X, YAN H, et al. Xiaoxianggou attenuates atherosclerotic plaque formation in endogenous high Ang II ApoE(-/-) mice via the inhibition of miR-203 on the expression of Ets-2 in endothelial cells [J]. Biomed Pharmacother, 2016, 82: 173–9.
6. ZHANG X, LV H, LI Z, et al. HPLC/QTOF-MS/MS application to investigate phenolic constituents from Ficus pandurata H. aerial roots [J]. Biomed Chromatogr, 2015, 29(6): 860–8.
7. LIU Y, WEI F, WANG X, et al. Progress on biological activities of polyphenols [J]. Chinese Journal of Pharmaceuticals, 2021, 52(04): 471–83.
8. DALBETH N, GOSLING A L, GAFFO A, et al. Gout [J]. Lancet, 2021, 397(10287): 1843–55.
9. HUANG Y, YANG K, CHEN S, et al. Practice guideline for patients with hyperuricemia/gout [J]. Chinese Journal of Internal Medicine, 2020, 59(7): 519–27.
10. TAYLOR W J, FRANSEN J, JANSEN T L, et al. Study for updated Gout classification criteria: identification of features to classify Gout [J]. Arthritis Care Res (Hoboken), 2015, 67(9): 1304–15.

11. ASHIQ K, BAJWA M A, TANVEER S, et al. A comprehensive review on gout: The epidemiological trends, pathophysiology, clinical presentation, diagnosis and treatment [J]. J Pak Med Assoc, 2021, 71(4): 1234–8.
12. RENAUDIN F, ORLIAGUET L, CASTELLI F, et al. Gout and pseudo-gout-related crystals promote GLUT1-mediated glycolysis that governs NLRP3 and interleukin-1β activation on macrophages [J]. Ann Rheum Dis, 2020, 79(11): 1506–14.
13. BAUERNFEIND F G, HORVATH G, STUTZ A, et al. Cutting edge: NF-kappaB activating pattern recognition and cytokine receptors license NLRP3 inflammasome activation by regulating NLRP3 expression [J]. J Immunol, 2009, 183(2): 787–91.
14. LI D. Effects of Sinomenine combined with total glucosides of paeonyon expression of MyD88,NF-kappaB,ASC and Caspase-1 in RAW264.7 macrophages induced by monosodium urate crystal [D];Hebei, Hebei Medical University, 2017.
15. JING X. Study on the mechanism of total flavonoids of smilax glabra roxb. in treatment of gouty arthritis based on NLRP3/ASC/Caspase-1 axis [D]; Zhejiang, Zhejiang University of Traditional Chinese Medicine, 2018.
16. FANG S. Research on the mechanism of Guizhishaoyaozhimu Decoction in treatment of gouty arthritis in rats via Toll-MyD88 and NLRP3 inflammasomes signaling pathway [D]; Hubei, Hubei University of Traditional Chinese Medicine, 2016.
17. SHEN R, MA L, ZHENG Y. Anti-inflammatory effects of luteolin on acute gouty arthritis rats via TLR/MyD88/NF-κB pathway [J]. Zhong Nan Da Xue Xue Bao Yi Xue Ban, 2020, 45(2): 115–22.
18. JABLONSKI K, YOUNG N A, HENRY C, et al. Physical activity prevents acute inflammation in a gout model by downregulation of TLR2 on circulating neutrophils as well as inhibition of serum CXCL1 and is associated with decreased pain and inflammation in gout patients [J]. PLoS One, 2020, 15(10): e0237520.
19. LIANG H, ZHANG Y, XIE J, et al. Advances in herbal treatment of acute gouty arthritis [J]. Journal of Emergency in Traditional Chinese Medicine, 2019, 28(03): 553–6.
20. ZHANG X, ZENG H, LI H, et al. Pathogenesis of gouty arthritis and intervention with Chinese medicines: A Review [J]. Chinese Journal of Experimental Traditional Medical Formulae, 2022, 28(11): 256–67.
21. JIAN R, YANG M, ZHENG S, et al. Requlatory effect of berberine on NLRP3/TLRs in mice with gouty arthritis [J]. Journal of Chongqing Medical University, 2020, 45(02): 251–6.
22. ZHANG R, ZHAN S, LI S, et al. Anti-hyperuricemic and nephroprotective effects of extracts from Chaenomeles sinensis (Thouin) Koehne in hyperuricemic mice [J]. Food Funct, 2018, 9(11): 5778–90.
23. WEI A, YUAN M, LIU J, et al. Research progress on application and mechanism of traditional Chinese medicine in Gout [J]. Chinese Journal of Experimental Traditional Medical Formulae, 2020, 26(19): 225–34.

24. ZHU H, MA R, YU K, et al. Clinical observation of floating acupuncture combined with traditional She medicine Xiaoxianggou for acute gouty arthritis [J]. New Chinese Medicine, 2018, 50(07): 211–4.
25. ZHANG W, LI A, LI K, et al. Progress on pharmacodynamic material basic of traditional Chinese medicine [J]. Chinese Pharmaceutical Journal, 2018, 53(10): 761–4.
26. FENG J, HUANG X, LI H, et al. Mechanism of resveratrol inhibiting monosodium urate induced oxidative damage ofRAW264.7 macrophages [J]. Acta Pharmaceutica Sinica, 2020, 55(10): 2368–74.
27. HSIN K Y, GHOSH S, KITANO H. Combining machine learning systems and multiple docking simulation packages to improve docking prediction reliability for network pharmacology [J]. PLoS One, 2013, 8(12): e83922.
28. ZHONG Z, LI Y, CHEN Y, et al. Predicting and exploring the mechanisms of Erzhi Pill in prevention and treatment of osteoporosis based on network pharmacology and zebrafish experiments [J]. Drug Des Devel Ther, 2021, 15: 817–27.
29. CHEN C, MIAO Y, LI H, et al. Prediction of quality markers of flavonoid components of Xinhui Chenpi based on UPLC.MS/MS compositional analysis combined with network pharmacology [J]. Global Traditional Chinese Medicine, 2022, 15(03): 417–26.
30. ZHU X, SUN Y, ZHANG C, et al. Effects of berberine on a rat model of chronic stress and depression via gastrointestinal tract pathology and gastrointestinal flora profile assays [J]. Mol Med Rep, 2017, 15(5): 3161–71.
31. MARTINS DE Sá MüLLER C, COELHO G B, CAROLINA DE PAULA MICHEL ARAúJO M, et al. Lychnophora pinaster ethanolic extract and its chemical constituents ameliorate hyperuricemia and related inflammation [J]. J Ethnopharmacol, 2019, 242: 112040.
32. LODHI S, VADNERE G P, PATIL K D, et al. Protective effects of luteolin on injury induced inflammation through reduction of tissue uric acid and pro-inflammatory cytokines in rats [J]. J Tradit Complement Med, 2020, 10(1): 60–9.
33. GAN B, LI H, ZHANG X, et al. Research progress in the treatment of gouty arthritis with traditional Chinese medicine nonomer [J]. China Journal of Traditional Chinese Medicine and Pharmacy, 2022, 37(10): 5848–52.
34. WANG Y, ZHOU T, WU S, et al. Research progress of polyphenols in cherry [J]. China Fruit & Vegetable, 2021, 41(10): 9–15 + 21.
35. SONG J, CHU F, WANG P, et al. Situation and Prospect of Research on Potential Basis of Chinese Medicine [C]. The Eighth Annual Conference of Chinese Medicine Chemistry Branch, Chinese Society of Traditional Chinese Medicine., Beijing, CHINA, F, 2013.
36. A L H C X Z E. Development and validation of bioacive components of Xaoxanggou (Ficus)[J]. CNWANC mroceedings of the 2014 intermnationa conterence on Medicine Sciences and Bioengineering London: CRC Press, 2015:231–236.SONG
37. YAN X, WANG Z, WANG G, et al. Research progress on extraction of polyphenols from pomegranate pee [J]. Shandong Chemical Industry, 2022, 51(24): 79–80 + 3.

38. LI B, LEI Y, MENG X, et al. Optimization of ultrasonic-assisted extraction of polyphenols from haskap berries (Loniceracaerulea L.) using response surface methodology and their antioxidant capacity [J]. Food Science, 2015, 36(22): 33–9.
39. YING Y. Analysis of the nutritional components and study of total flavonoids in Xiaoxianggou [D]; Zhejiang, Zhejiang University, 2012.
40. ZHOU F, MEI J, HAN X, et al. Kinsenoside attenuates osteoarthritis by repolarizing macrophages through inactivating NF-κB/MAPK signaling and protecting chondrocytes [J]. Acta Pharm Sin B, 2019, 9(5): 973–85.
41. LI S, LI L, YAN H, et al. Anti–gouty arthritis and anti–hyperuricemia properties of celery seed extracts in rodent models [J]. Mol Med Rep, 2019, 20(5): 4623–33.
42. BOUSOIK E, QADRI M, ELSAID K A. CD44 receptor mediates urate crystal phagocytosis by macrophages and regulates inflammation in A Murine peritoneal model of acute Gout [J]. Sci Rep, 2020, 10(1): 5748.
43. PELEGRIN P, BARROSO-GUTIERREZ C, SURPRENANT A. P2X7 receptor differentially couples to distinct release pathways for IL-1beta in mouse macrophage [J]. J Immunol, 2008, 180(11): 7147–57.
44. GUO M, OUYANG X, WANG L, et al. Effects of plantamajoside, Tricin,and Chrysoeriol on the inflammation model of RAW264.7 macrophages induced by sodium urate crystals [J]. Pharmacology and Clinics of Chinese Materia Medica, 2022, 38(02): 49–53.
45. LI Z, LI D, MA X, et al. Effects of Sinomenine combined with total glucosides of paeonyon expression of MyD88, NF-kappaB,ASC and Caspase-1 in RAW264.7 macrophages induced by monosodium urate crystal [C]. Compendium of Abstracts of the 12th National Congress of Immunology, F, 2017.
46. FENG J, LIU Y, HAO R, et al. Ethanol extract of siegesbeckiae herba intervening gouty arthritis via regulating TLRs/NFKB signaling pathway and NLRP3 [J]. Traditional Chinese Drug Research and Clinical Pharmacology, 2020, 31(03): 264–9.
47. CODERRE T J, WALL P D. Ankle joint urate arthritis in rats provides a useful tool for the evaluation of analgesic and anti-arthritic agents [J]. Pharmacol Biochem Behav, 1988, 29(3): 461–6.
48. LV J, FANG H, WU T, et al. Study of a modified acute gouty arthritis rat model [J]. China Journal of Modern Medicine, 2014, 24(18): 17–21.
49. SONG J, LI Q, ZHANG Q, et al. Preparation of gouty arthritis model in rats by modified method [J]. China Modern Medicine, 2018, 25(31): 4–6.
50. CAI T, WANG X, HE Z, et al. Establishment of a rat model of acute gouty arthritis and observation of the model maintenance time [J]. Acta Laboratorium Animalis Scientia Sinica, 2017, 25(05): 494–9.
51. HUANG H, SUN Y, HU M, et al. Characteristics of monosodium urate monohydrate crystal-induced acute arthritis in rats that mimicked human gouty arthritis [J]. Military Medical Sciences, 2005, (06): 538–42.
52. JOOSTEN L A, ABDOLLAHI-ROODSAZ S, DINARELLO C A, et al. Toll-like receptors and chronic inflammation in rheumatic diseases: new developments [J]. Nat Rev Rheumatol, 2016, 12(6): 344–

57.

53. ZHAO L, YE W, ZHU Y, et al. Distinct macrophage polarization in acute and chronic gout [J]. Lab Invest, 2022, 102(10): 1054–63.
54. BAILEY K N, FURMAN B D, ZEITLIN J, et al. Intra-articular depletion of macrophages increases acute synovitis and alters macrophage polarity in the injured mouse knee [J]. Osteoarthritis Cartilage, 2020, 28(5): 626–38.
55. JIA P, CHEN G, YANG J et al. Study on the effect of Simiao Pills on inflammation development and regulation of macrophage polarization in rats with gouty arthritis [J]. China Journal of Traditional Chinese Medicine and Pharmacy, 2022, 37(06): 3498–502.
56. LIU L, ZHU X, ZHAO T, et al. Sirt1 ameliorates monosodium urate crystal-induced inflammation by altering macrophage polarization via the PI3K/Akt/STAT6 pathway [J]. Rheumatology (Oxford), 2019, 58(9): 1674–83.

# Figures

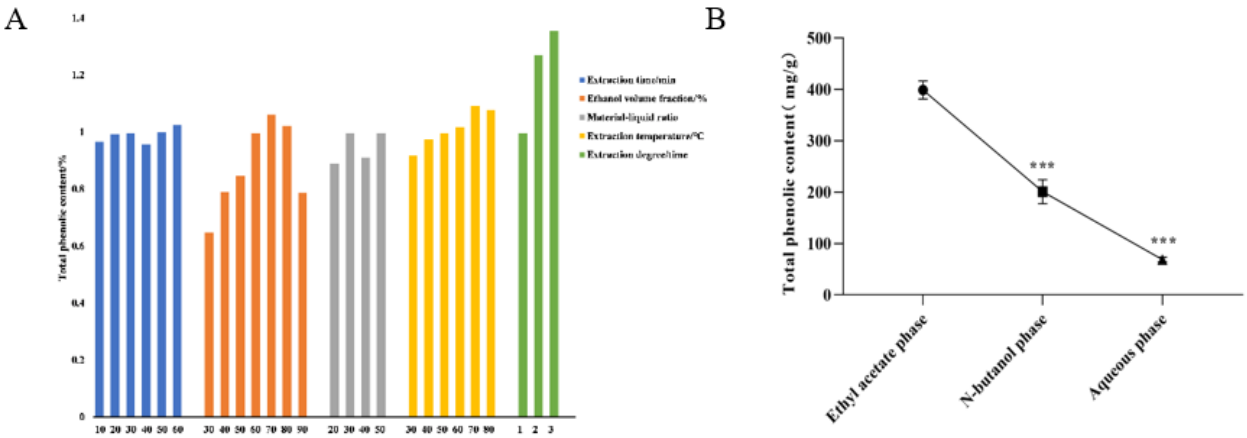


**Figure 1**

Total phenol yield of Xiaoxianggou under different extraction conditions(A). Total phenol content of extracts from various phases of Xiaoxianggou(B).Total phenol content of extracts from various phases of Xiaoxianggou was determined using Folin-Ciocalteau method. $^{***}P<0.001$, compared to ethyl acetate phase of Xiaoxianggou.

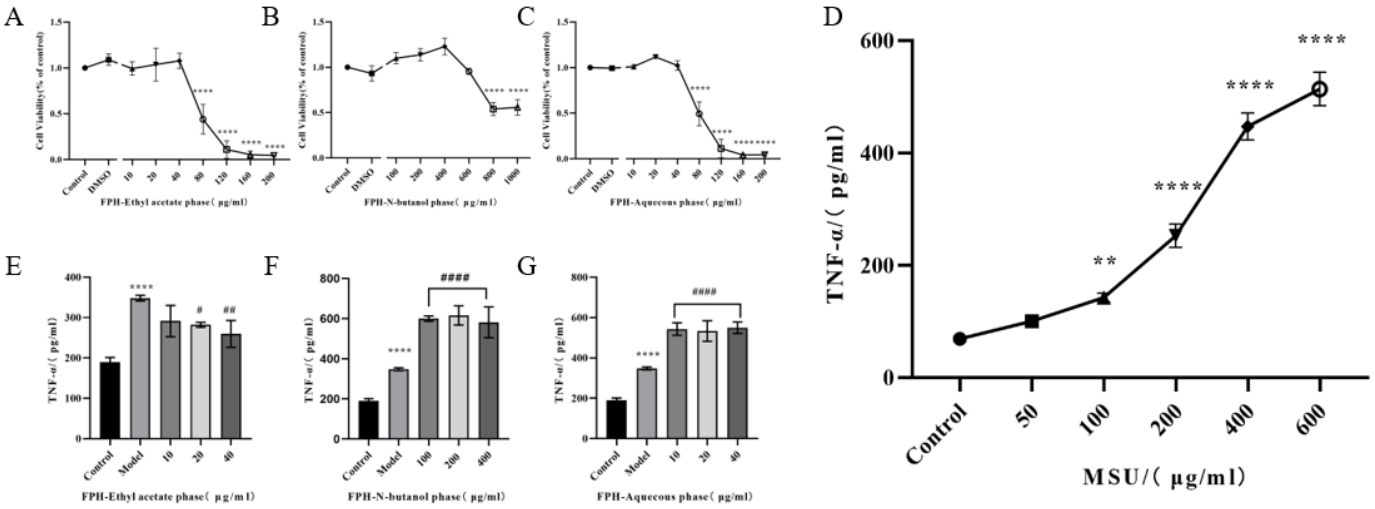


## Figure 2

Cytological screening of the effective parts of the Xiaoxianggou. The ethyl acetate phase (A), n-butanol phase (B) and aqueous phase (C) of Xiaoxianggou intervened RAW264.7 cells for 24h, and the cell viability was measured by MTS method. Sodium urate interfered with macrophages for 24h, and TNF-α expression was measured by ELISA. After the intervention of macrophages with ethyl acetate phase (C), n-butanol phase (D) and aqueous phase (F) for 6h, sodium urate was added to stimulate the macrophages for 24h, and TNF-α expression was measured by ELISA.$^{*}P$<0.05, $^{**}P$<0.01, $^{****}P$<0.0001 compared to control group.$^{\#}P$<0.05, $^{\#\#}P$<0.01, $^{\#\#\#\#}P$<0.0001 compared with model group.

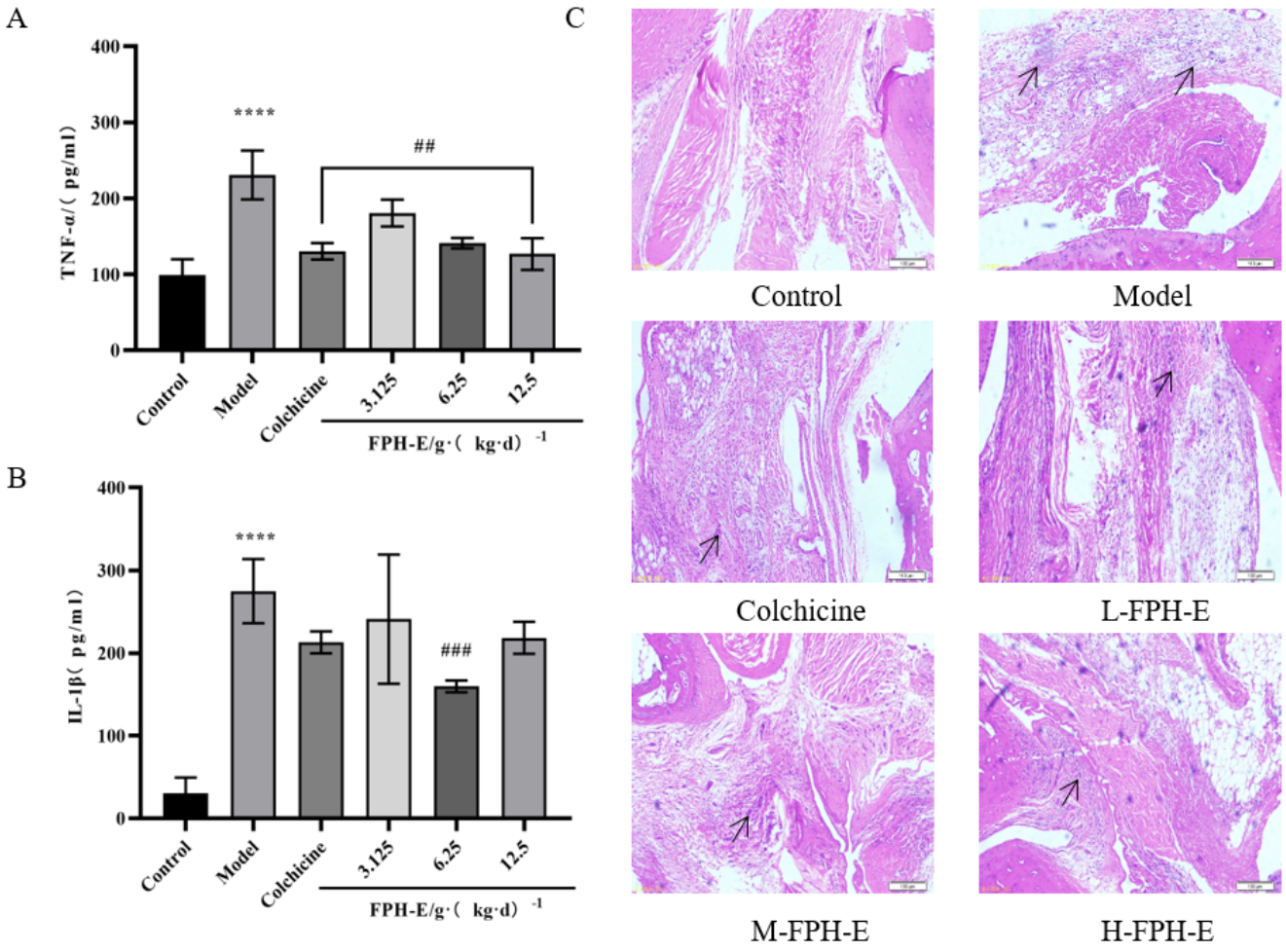


## Figure 3

Therapeutic effect of Xiaoxianggou ethyl acetate active part on GA rats. Except for the control group, 100 μL MSU solution (25 mg/mL) was injected into the ankle joint of each group of rats. Colchicine 0.3 mg/kg was given to the positive control group, and different concentrations of Xiaoxianggou ethyl acetate effective part were given to the drug treatment group. ELISA was used to detect the expressions of TNF-α (A), IL-1β (B)in rats ankle joint. Pathological tissue changes of rat ankle joints were observed by HE staining (C). $^{****}P<0.0001$ compared to control group. $^{\#\#}P<0.01$, $^{\#\#\#}P<0.001$, compared with model group.

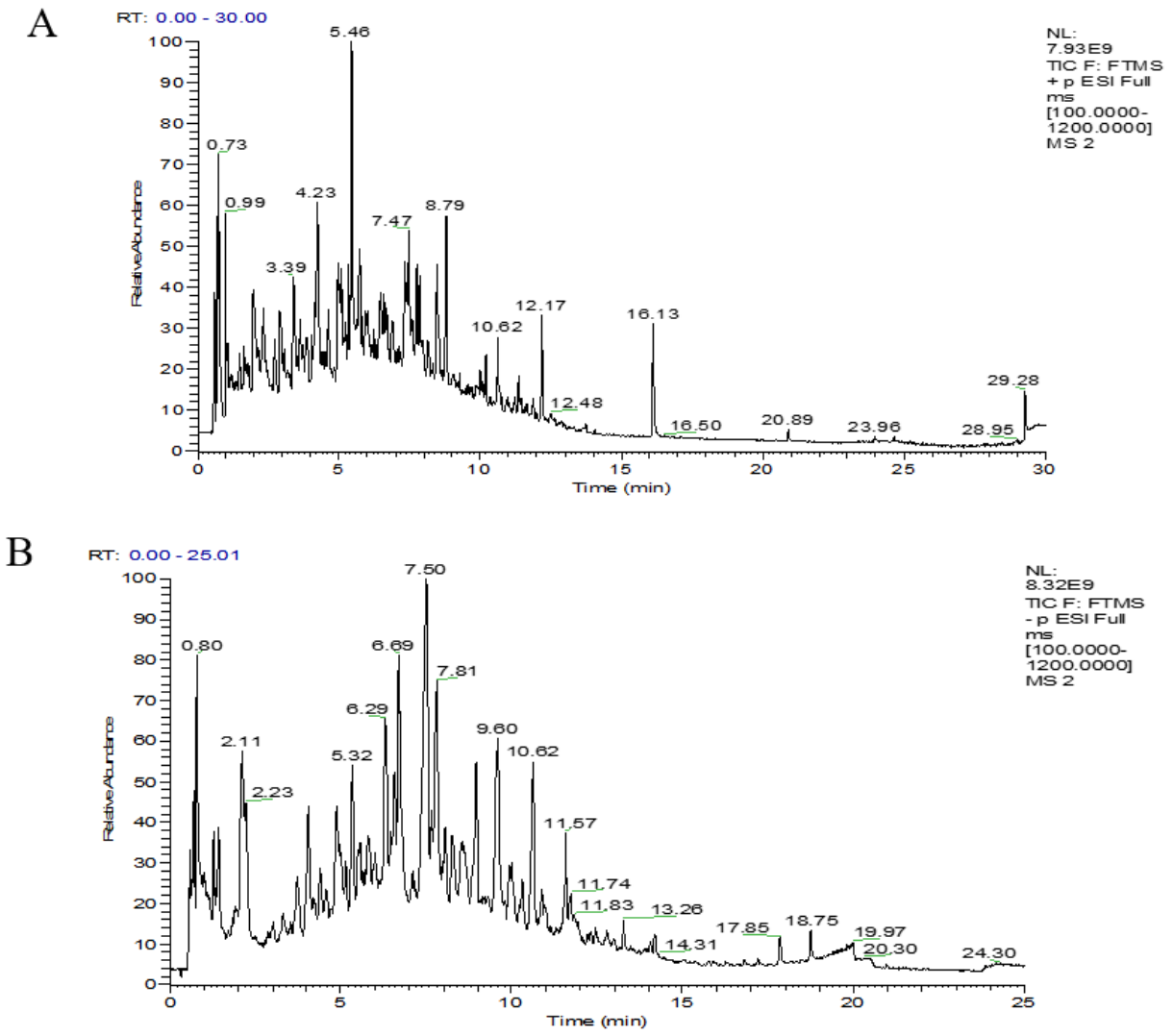


## Figure 4

LC-MS/MS map of lyophilized powder at the Xiaoxianggou ethyl acetate effective part. Total ion flow diagram in positive ion mode (A). Total ion flow diagram in Negative ion mode (B).

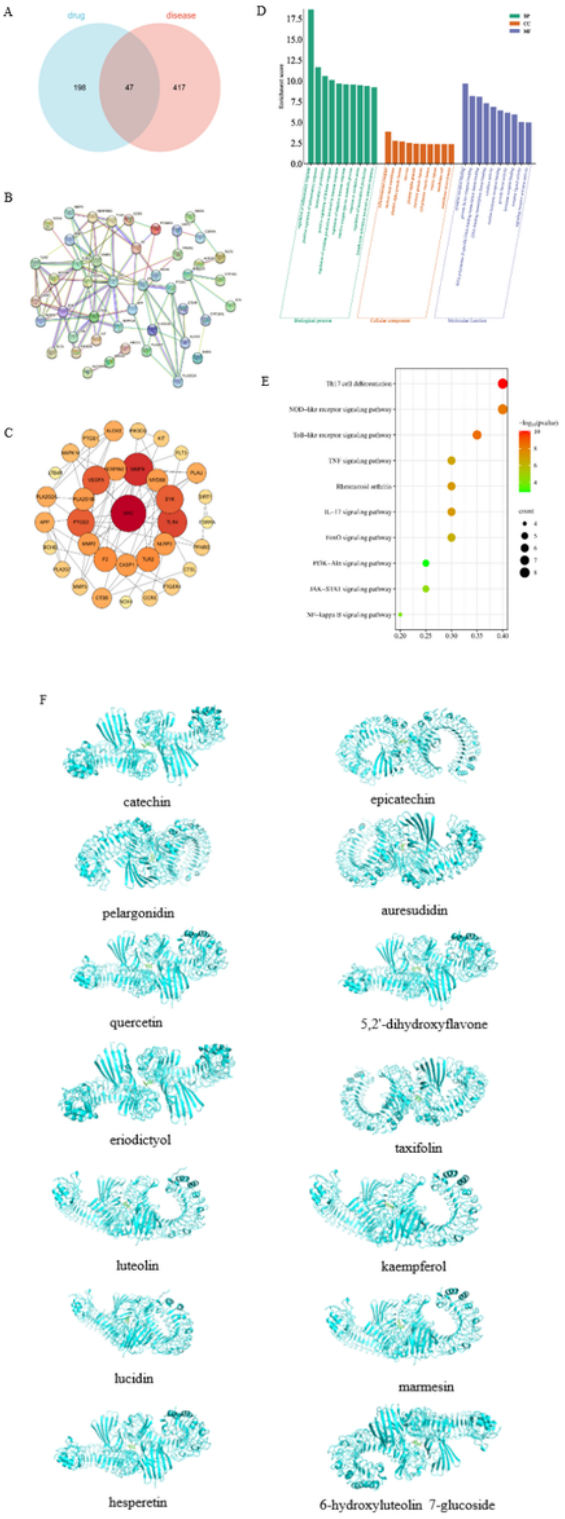


## Figure 5

Venn diagram of the intersection of each active ingredient of Xiaoxianggou ethyl acetate effective part with GA gene (A). Protein interaction network diagram (B) and drug target modulation network (C) of Xiaoxianggou ethyl acetate effective part for GA treatment. GO functional was performed on the screened 47 target genes highly related to GA (D). The figure shows the top 10 GO terms in biological regulation (BP, green), cellular component (CC, orange), and molecular function (MF, purple) respectively. KEGG

enrichment analysis of the signaling pathways that the differently expressed genes may be involved in, the size of the dots indicates the number of differential genes annotated to the pathway, and the color indicates the adjusted P value (E). Molecular docking pattern of Xiaoxianggou potential active component to TLR-4 target proteins (F).

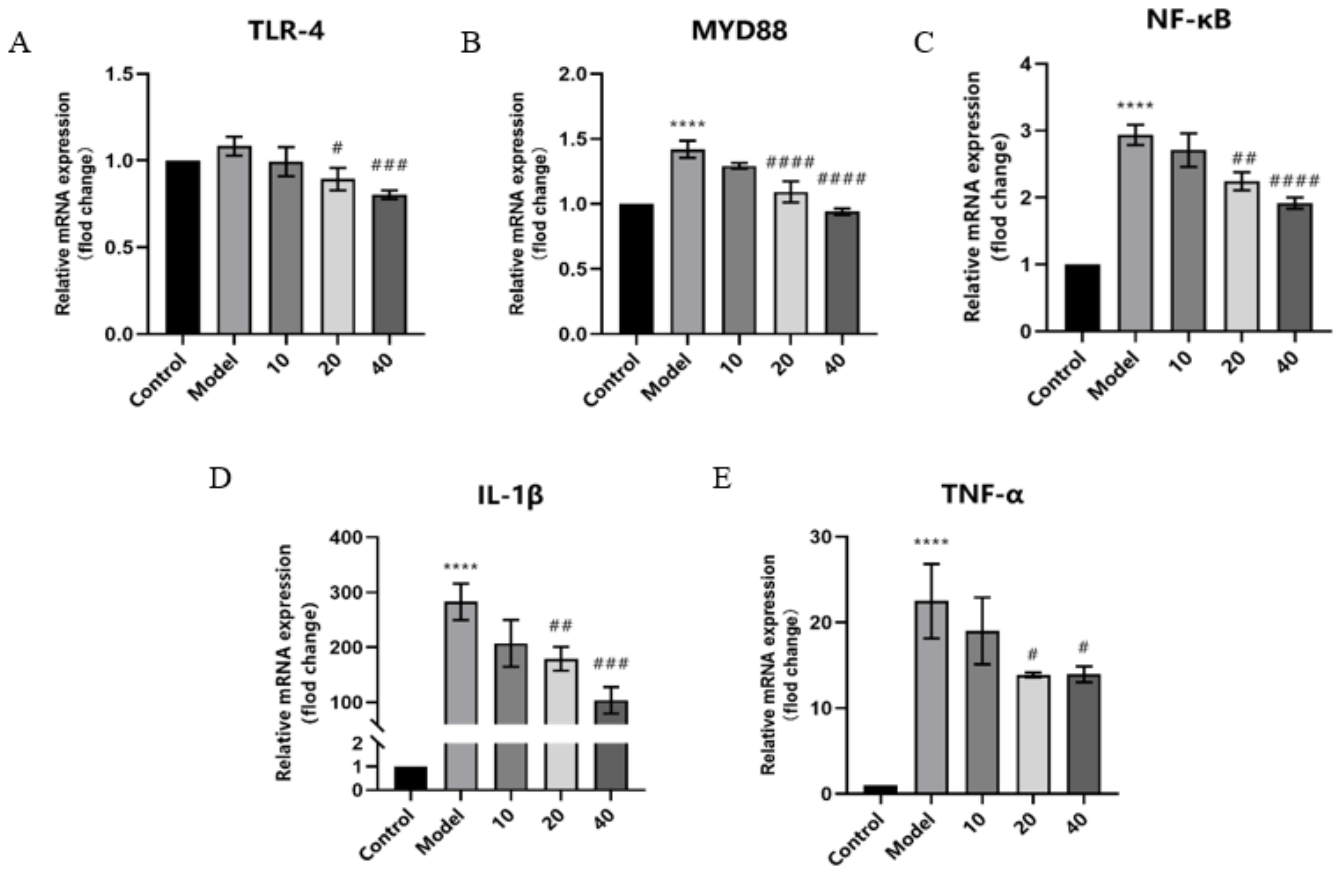


## Figure 6

Xiaoxianggou ethyl acetate effective part reduced the level of *TLR4 MYD88 NF-κB TNF-α IL-1β* produced by RAW264.7 cell. After treatment with different concentrations of Xiaoxianggou ethyl acetate effective part (10,20,40 μg/mL) for 6 h, RAW264.7 cell was incubated with 400 μg/mL MSU. The mRNA expressions of *TLR4 MYD88 NF-κB TNF-α IL-1β* in RAW264.7 cells in each group were detected by qRT-PCR. $^{****}P<0.0001$ compared to control group. $^{\#}P<0.01$, $^{\#\#}P<0.01$, $^{\#\#\#}P<0.001$, $^{\#\#\#\#}P<0.0001$compared with model group.